Skeletal Radiol (2000) 29:680–689
© International Skeletal Society 2000

ARTICLE

**Jin-Suck Suh**
**Jaemin Cho**
**Sang Hoon Lee**
**Kyoo-Ho Shin**
**Woo Ick Yang**
**Jeong Hoon Lee**
**Jae-Hyun Cho**
**Kyung Jin Suh**
**Young Joon Lee**
**Kyung Nam Ryu**

# Alveolar soft part sarcoma: MR and angiographic findings

Received: 12 April 2000
Revision requested: 27 June 2000, 8 August 2000
Revision received: 2 August 2000, 21 August 2000
Accepted: 22 August 2000

J.-S. Suh (✉), J. Cho, S.H. Lee
Department of Diagnostic Radiology, College of Medicine Yonsei University, #132 Shinchondong, Seodaemoon-gu, Seoul, 120–752, Korea

K.-H. Shin
Department of Orthopaedic Surgery, College of Medicine Yonsei University, Korea

W.I. Yang
Department of Pathology, College of Medicine Yonsei University, Korea

J.H. Lee
Department of Diagnostic Radiology, Korea Cancer Center Hospital, Korea

J.-H. Cho
Department of Diagnostic Radiology, Ajou University, Korea

K.J. Suh
Department of Diagnostic Radiology, Kyungpook National University, Korea

Y.J. Lee
Department of Diagnostic Radiology, In Je University, Korea

K.N. Ryu
Department of Diagnostic Radiology, Kyung Hee University, Korea

**Abstract** *Objective*. To present the MR and angiographic findings of alveolar soft part sarcoma (ASPS).
*Design and patients*. MR examinations (12 tumors of 10 patients) of ASPS performed at multiple hospitals were retrospectively reviewed. The tumors were found in the thigh (*n*=4), lower leg (*n*=4), femur (*n*=2, local metastasis), scalp (*n*=1) and arm (*n*=1). The MR signal characteristics including signal intensity, homogeneity and signal void of lesions and bony invasion including direct invasion or local metastasis were evaluated. Angiographic findings (*n*=4) and post-embolotherapy follow-up MR imaging (*n*=2) findings were also assessed.
*Results*. Local bony metastasis was found in two cases. Seven tumors showed heterogeneous high signal intensity on T1- and T2-weighted images with good enhancement. One tumor had a very high signal on T1-weighted images. Eight tumors (67%) showed numerous signal voids in or near the tumors. All four angiographic studies showed numerous enlarged vessels, arteriovenous shunts and delayed washout. Two cases mimicked arteriovenous malformations on angiographic studies but MR images demonstrated solid soft tissue components as well as tortuous vessels.
*Conclusions*. High signal on T1-weighted image and numerous signal voids are highly suggestive of ASPS, although they are not universal as has been suggested and arteriovenous malformation should be included in the differential diagnosis. Local bony metastases in ASPS were seen in two cases and should be carefully investigated.

**Keywords** Sarcoma · Soft tissues · Neoplasm · Soft tissues · MR imaging

www.manaraa.com

## Introduction

Alveolar soft part sarcoma (ASPS) is a morphologically distinct malignant soft tissue sarcoma which was initially described by Christopherson et al. [1]; its histogenesis is uncertain. Radiologists may not be familiar with the imaging findings as these tumors are rare, comprising approximately 0.5–1% of all soft tissue sarcomas [2]. As ASPS is slow growing, symptoms are uncommon and patients and physicians can overlook the tumor. Recently, investigators have reported that high signal intensity on T1- and T2-weighted images and flow voids [3, 4] are characteristic MR findings of ASPS. However, the signal intensity changes of ASPS are not specific and flow voids are also not pathognomonic. ASPS is an extremely vascular tumor, which may present as a pulsatile mass with an audible bruit, and can mimic arteriovenous malformations. In these circumstances suspicion of ASPS will result in tissue biopsy, which will avoid inappropriate therapy such as embolotherapy, a current principal treatment method for arteriovenous malformations. Local bone metastases in ASPS have only recently been addressed in imaging studies, and this may be an important issue for local tumor management. We have therefore reviewed the MR findings of ASPS and correlated the angiographic findings in selected cases.

## Materials and methods

MR imaging of 10 patients with 12 pathologically proven ASPS were retrospectively reviewed. Histological preparation was undertaken with hematoxylin and eosin staining in all cases and supplemented with PAS stain in seven cases. MR studies were available in all cases and angiography in four patients. In four patients, follow-up MR imaging was performed after preoperative chemotherapy and embolotherapy ($n$=2) or preoperative chemotherapy alone ($n$=2). Selective arterial embolization was performed with polyvinyl alcohol foam powder with gelatin sponge. All available imaging studies were retrospectively reviewed for the evidence of metastatic disease. MR was performed at five institutions using 1.5-T (Signa Advantage, GE Medical Systems, Milwaukee, Wis.; Magnetom, SP 4000, Siemens Medical Systems, Iselin, N.J.) or 0.5-T scanners (Gyroscan T5, Philips Medical Systems, Best, The Netherlands). In all cases, T1-weighted images (TR/TE = 350–700/10–20), T2-weighted images (2200–3500/60–80), and T1-weighted images after intravenous administration of 0.1 mmol/kg body weight of gadopentetate dimeglumine (Magnevist; Berlex Laboratories, Wayne, N.J.; Schering, Berlin, Germany) were obtained. Typical MR imaging parameters were as follows: field of view, 16–35 cm; one or two acquisitions; matrix size, 256×192; section thickness, 5–10 mm; intersection gap, 3–5 mm.

We reviewed the MR images for signal intensity, signal homogeneity, and the presence of flow voids, osseous invasion and contrast enhancement. Muscle was used as the normal reference tissue on T1-weighted images, and subcutaneous fat was used as the normal reference tissue on T2-weighted images. Digital subtraction angiography was performed using a transfemoral approach with a 5 Fr catheter. Angiography was reviewed from the viewpoint of vascularity, arteriovenous shunt and washout delay. Skeletal scintigraphy was performed in all but three patients (nos. 2, 8, 9) and distant or local metastases were assessed. Chest CT scan was undertaken in seven cases at initial diagnosis.

## Results

The clinical data of the patients are summarized in Table 1. There were three male and seven female patients (age range 17–48 years, mean age 29 years). They presented with either a mass ($n$=8) or pain ($n$=2). Eight patients had a single soft tissue tumor and two had a soft tissue mass and local bony metastatic lesions. The tumors were in the thigh ($n$=4), lower leg ($n$=4), femur ($n$=2, local metastasis), scalp ($n$=1) and arm ($n$=1). Histological examinations were undertaken on all patients and demonstrated a pseudoalveolar pattern and nests of tumor cells separated by sinusoidal vascular channels and individual cells with vesicular nucleoli and abundant eosinophilic cytoplasm. Whole-body bone scintigraphy was undertaken in eight cases; in two cases (nos. 2, 8) it was not undertaken or the data lost. Three cases showed bone metastases at initial presentation, which were distant in two cases. Plain radiographs and CT scans of the chest were available in seven cases. Six of these showed metastasis in the lungs. In three cases (nos. 2, 8, 10), chest CT was not performed at the initial investigation, but two (nos. 2, 8) had lung metastatic lesions detected on the chest radiograph and one (no. 10) did not show metastatic lesions at initial diagnosis. Overall seven patients had metastatic lesions in the lungs at initial presentation and two developed them during the follow-up period. One patient was died during follow-up and two were lost; the mean duration of follow-up was 17 months.

Local bone metastases were found in two patients. One female patient presenting with pain in the distal femur (no. 4) had a tumor in the medial femoral condyle and two further nodules in the femur. A primary tumor was later demonstrated in the left calf during angiography, which was asymptomatic (Fig. 1). Whole-body bone scintigraphy did not reveal any metastatic bone lesion except in the distal femur. A further patient (no. 5) had a local metastasis in the proximal femur, from a primary mass in the anterior, upper thigh (Fig. 2). This patient had direct tumor invasion into the acetabulum and a skip nodular lesion in the ischial ramus. Again histological examinations revealed a characteristic pseudoalveolar pattern and nests of tumor cells separated by sinusoidal vascular channels (Figs. 1, 2). Individual cells showed vesicular nucleoli and abundant eosinophilic cytoplasm. Tumor emboli were found in the vessels (Fig. 2). Direct bone invasion was also found in two other patients (Fig. 3).

MR appearances are summarized in Table 2. Most tumors showed heterogeneously high signal intensity on T1-weighted and T2-weighted images. The tumors were enhanced, either homogeneously (40%) or heterogeneously (60%). Seven showed numerous round or ser-

www.manaraa.com

**Table 1** Clinical data of the patients (*NA* not available for further analysis for the subtype or character)

| Case no. | Sex | Age (years) | Chief complaints | Location | Treatment | Pathologic review[a] | Initial presentation distant metastasis | Outcome |
|---|---|---|---|---|---|---|---|---|
| 1 | F | 20 | Mass | Semimembranosus | Embolization, chemotherapy, excision | Biopsy, characteristic; excision, extensive tumor necrosis | None | 29 months – alive; 27 months – lung metastasis |
| 2 | F | 29 | Pain | Triceps, deltoid | Nil | NA | Lung, brain | Lost |
| 3 | F | 30 | Mass | Soleus | Nil | Characteristic | Lung | 8 months – alive |
| 4 | F | 39 | Asymptomatic | Soleus, gastrocnemius | Chemotherapy, excision | Characteristic | Lung, bone | 15 months – alive |
| | | | Pain | Femur[b] | Curettage, chemotherapy | Characteristic, and hemorrhagic, dilated veins, and crystals | | |
| 5 | F | 26 | Mass | Thigh adductors, pectineus | Chemotherapy, excision, radiotherapy | Characteristic, and hemorrhagic, intravenous tumor thrombi | Lung, bone | 19 months – alive |
| | | | Asymptomatic | Femur[b] | Chemotherapy | Not done | | |
| 6 | M | 24 | Mass | Scalp | Chemotherapy | Characteristic, crystals | Lung, bone | Died at 6 months |
| 7 | F | 23 | Mass | Vastus intermedius | Embolization, chemotherapy, radiotherapy | NA | Lung | 24 months – alive; 11 months – bone metastasis |
| 8 | F | 48 | Mass | Peroneus | Nil | NA | Lost | Lost |
| 9 | M | 37 | Mass | Vastus lateralis and intermedius | Chemotherapy, Radiotherapy, excision | Characteristic | Lung | 20 months – alive |
| 10 | M | 17 | Mass | Gastrocnemius | Chemotherapy | Characteristic | None | 24 months – alive; 3 months – lung metastasis |

[a] "Characteristic" indicates pseudoalveolar pattern and nests of tumor cells separated by sinusoidal vascular channel and individual cells with vesicular nucleoli and abundant eosinophilic cytoplasm
[b] Local metastatic bone

www.manaraa.com

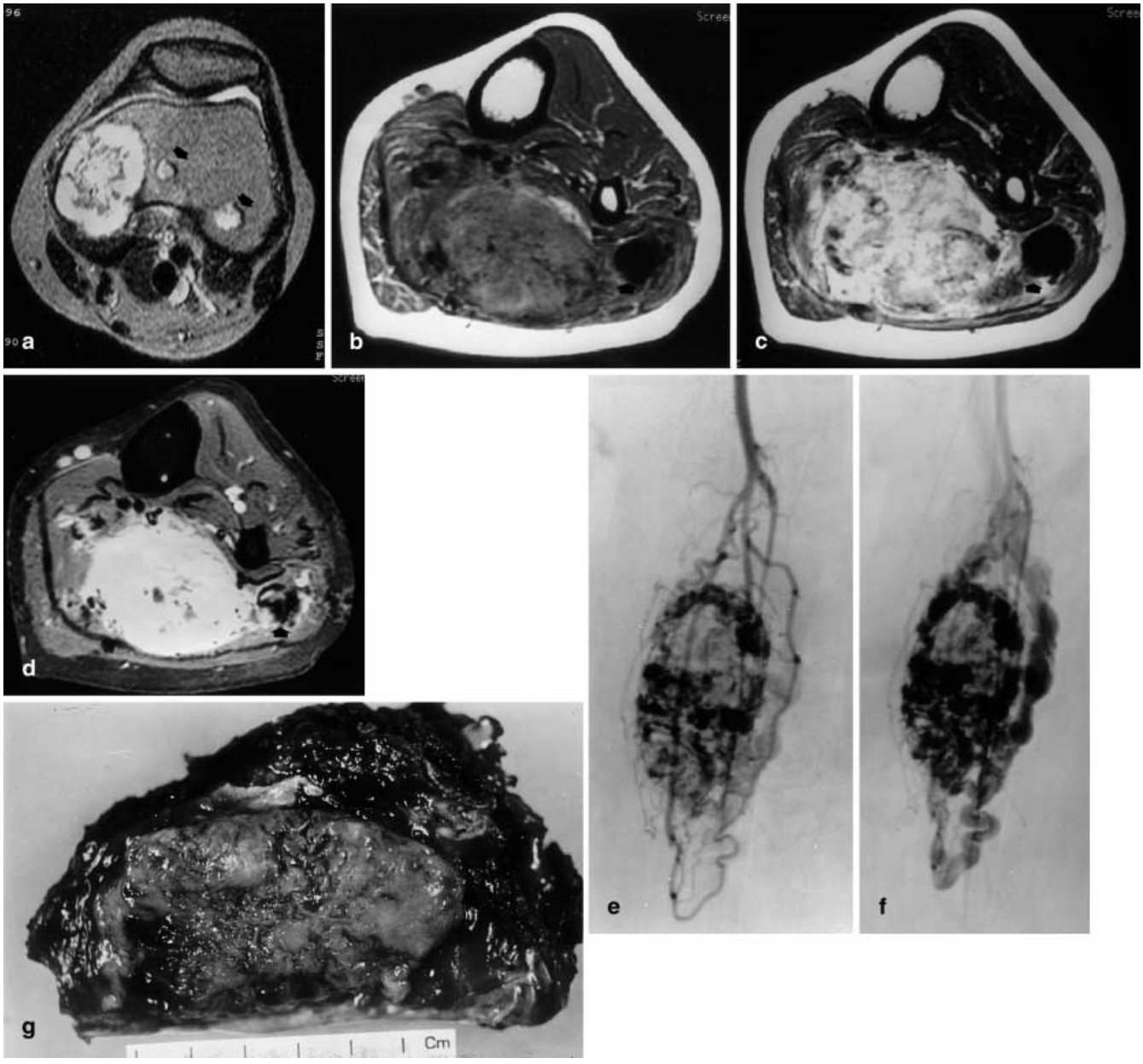


**Fig. 1a–i** Local bone metastases in the femur. **a** T2-weighted image shows a well-demarcated mass and two satellite nodules (*arrows*) in the medial femoral condyle. **b** T1-weighted image shows slightly increased signal, **c** T2-weighted image shows heterogeneously high signal and **d** T1-weighted fat-saturation post-contrast image shows strong enhancement in the mass of the calf. Numerous signal voids are present in the tumor and at the periphery with the largest (*arrows* in **b**–**d**) seen posterior to the fibula. **e** Early arterial phase image of digital subtraction angiogram demonstrates arteriovenous shunting and **f** the delayed phase image shows venous drainage and delayed washout. **g** Gross specimen shows a lobulated mass with multiple hemorrhagic foci and **h** H&E-stained microslide shows prominent dilated veins within fibrous trabeculae dividing the tumor into multiple compartments. **i** PAS stain with diastase shows typical intracytoplasmic crystalline inclusions (*arrows*)

pentine signal voids (Fig. 3). Signal voids were observed in the tumor and/or at the periphery of the tumors. In contrast to the primary ASPS, bony lesions either from metastasis or direct invasion rarely showed signal voids on MR imaging.

Angiography showed numerous enlarged vessels, arteriovenous shunts and delayed washout in all four cases (Figs. 1, 2). Angiographic studies of two patients (nos. 4, 7) were mistaken for arteriovenous malformations at the initial interpretation. However, these cases were found to have abundant solid soft tissue components on MR imaging.

MR imaging undertaken for follow-up evaluation showed no change in size and signal intensity of the tumors after preoperative chemotherapy alone ($n$=2). Che-

www.manaraa.com

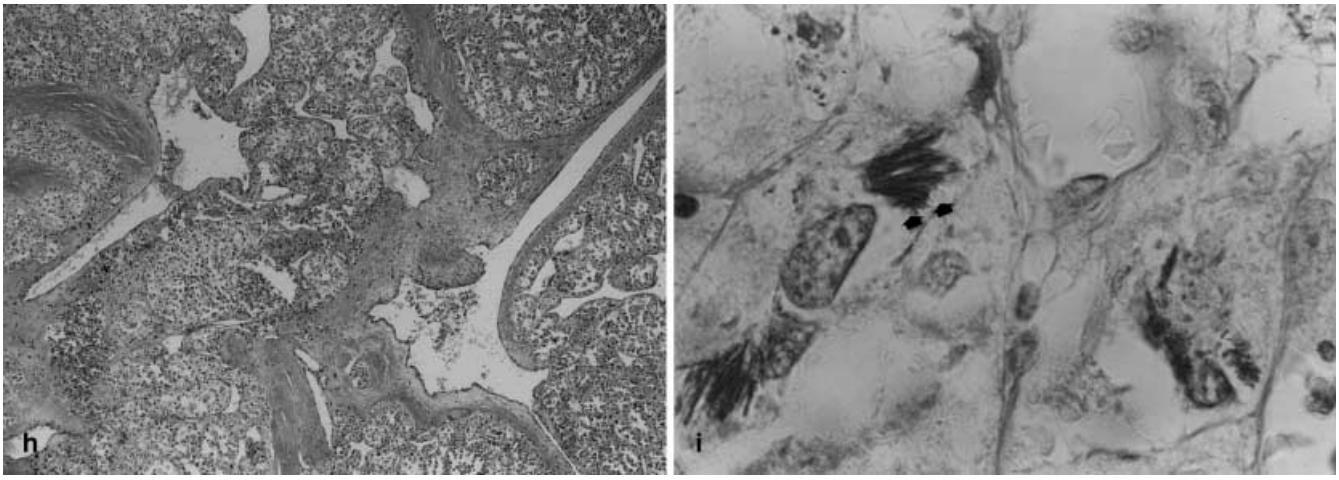


**Fig. 1h–i**

motherapy and embolotherapy (*n*=2) resulted in a varied response: in one patient the tumor showed extensive central necrosis (Fig. 4) while in the other it showed no change in size and signal intensity (Fig. 5).

## Discussion

ASPS predominantly affects young adults and females and frequently involves the lower extremities, but may develop in regions of the head and neck, particularly in children. In our study, one female patient presented with bone pain in the right distal femur, which was later found to be a local metastatic lesion. A primary mass in the calf was not accompanied by pain and was not detected until angiography was undertaken for the femoral lesion. Metastases are commonly demonstrated at initial presentation [5, 6] and involve the lung, bone and brain in that order of frequency. In our study, distant metastases were found in seven of ten patients at initial presentation. Median survival was 3–11 years with or without metastases at diagnosis in previous studies [5, 7]. Thus the presence of metastasis is a poor prognostic factor. In this study, the mean duration of follow-up was 17 months but the prognosis will probably be poor because metastases were present at diagnosis in 70% of patients.

Macroscopically, ASPS is usually a well-circumscribed mass with a homogeneous appearance on a cut surface. The microscopic picture is uniform, characterized by a pseudoalveolar pattern with nests of tumor cells separated by sinusoidal vascular channels [2]. Individual cells have vesicular nucleoli and abundant eosinophilic cytoplasm and show little variation. Periodic acid-Schiff (PAS) preparation frequently reveals rod- or sheaf-like crystals in the tumor cells, which is diagnostic of ASPS. Pathologically, the differential diagnosis includes metastatic renal cell carcinoma, alveolar rhabdomyosarcoma, paraganglioma and granular cell tumor. We did not perform genetic analysis but this tumor is known to have translocation t(X; 17)(p11.2; q25.3) [8].

A few investigators have described the radiological findings of ASPS and emphasized that ASPS has high signal on T1-weighted and T2-weighted images and multiple intra- and extra-tumoral signal voids [3, 4]. The high signal on T1-weighted sequence has been attributed to slow-flowing blood in or around the tumor [4, 9] or to chemotherapy [3]. In the review of our cases, signal intensity of the tumor on T1-weighted image was slightly higher than that of the muscles in most cases. Only one case (no. 3) showed very high serpentine signal, which was thought to be related to slow blood flow. However, many soft tissue sarcomas may show iso-intense or slightly increased signal on T1-weighted images. Clear cell sarcoma, metastatic melanoma, hemangioma, liposarcoma and soft tissue tumor with hemorrhage should be included in the differential diagnosis due to high signal intensity on T1-weighted images. Histologically, clear cell sarcoma has melanocytic differentiation, so T1 shortening is possible [10]. Multiple signal voids with a tubular appearance may relate to high blood flow and are frequently observed in ASPS. Such voids are not specific for ASPS either, but the combination of the high signal on T1-weighted images and signal void would suggest the diagnosis of ASPS. Clear cell sarcoma does not have the signal void on MR findings, and satellite nodule or local bone metastasis is rare. Hemangioma also has slightly high signal intensity on T1-weighted images due to fibrofatty components, and has signal void within high flow vessels [11].

Angiography showed highly vascular, arteriovenous shunts and delayed washout, which have also been described in previous reports [3, 4, 9]. On the basis of the angiographic findings, the differential diagnosis includes vascular malformations and highly vascularized soft tissue tumors [12]. Differentiation from arteriovenous malformation is very important [13] because arteriovenous

www.manaraa.com

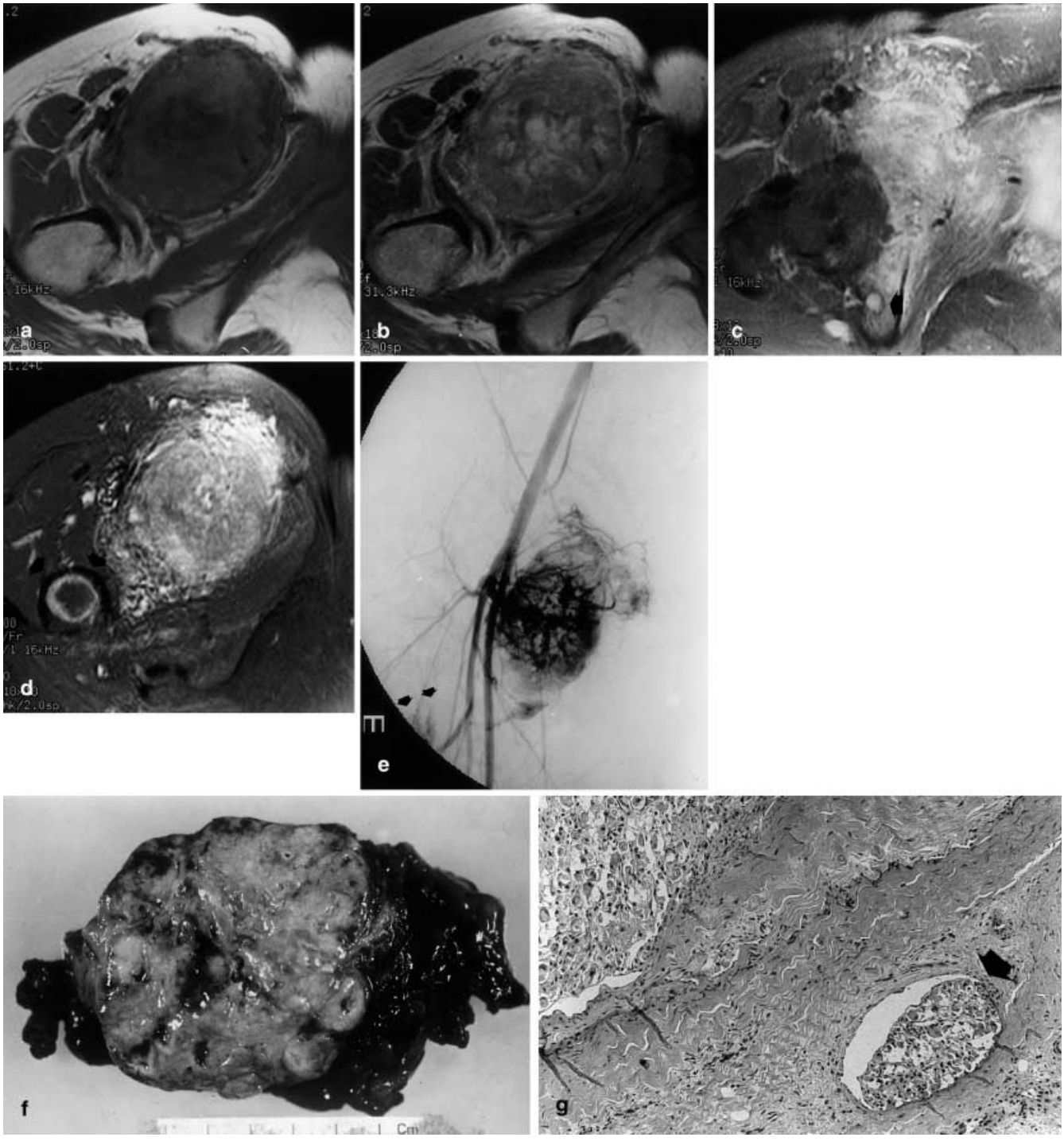


**Fig. 2a–g** Alveolar soft part sarcoma with direct bony invasion and local bone metastatic lesion. **a** T1-weighted and **b** T2-weighted images show a well-defined mass with heterogeneously high signal in the anterior, upper thigh and multiple signal voids at the periphery of the mass. **c**, **d** T1-weighted fat-saturation post-contrast images show a strongly enhancing mass which directly invades the acetabulum, extending to the internal obturator muscle. A skip lesion is seen in the ischium (**d**, *arrow*). Another bone lesion is demonstrated in the femur where intramedullary enhancement (**c**, *arrows*) is evident. **e** Angiography shows numerous tortuous enlarged vessels in the main mass at the early arterial phase but fewer vessels in the femoral lesion (*arrows*) and in the acetabular lesion. **f** Gross specimen of the incompletely excised soft tissue mass and acetabulum shows several hemorrhagic foci in the central portion of the mass. **g** Microscopic slide (H&E stain) shows a tumor embolus within a peripheral dilated vein (*arrow*)

www.manaraa.com

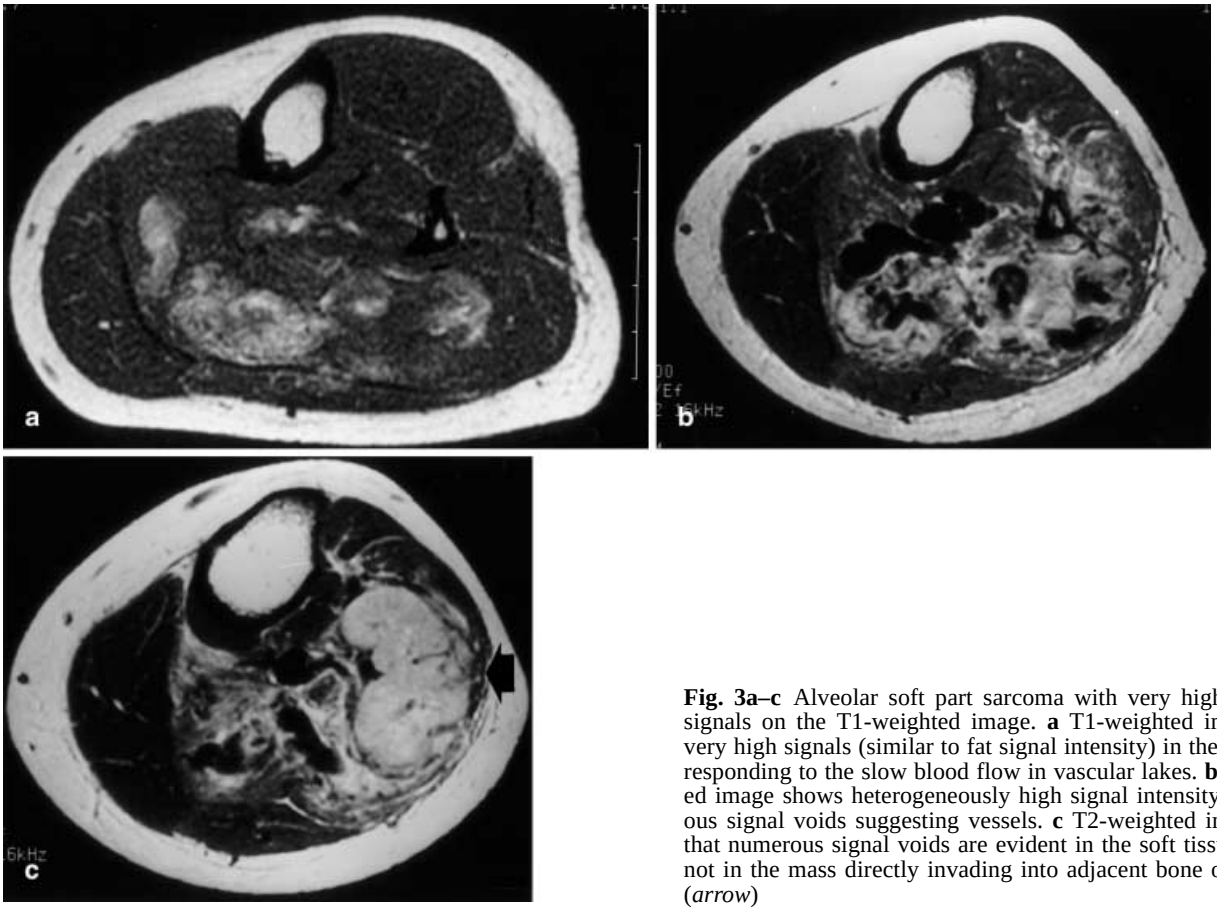


**Fig. 3a–c** Alveolar soft part sarcoma with very high serpentine signals on the T1-weighted image. **a** T1-weighted image shows very high signals (similar to fat signal intensity) in the tumor, corresponding to the slow blood flow in vascular lakes. **b** T2-weighted image shows heterogeneously high signal intensity with tortuous signal voids suggesting vessels. **c** T2-weighted image shows that numerous signal voids are evident in the soft tissue mass but not in the mass directly invading into adjacent bone of the fibula (*arrow*)

malformation is often treated with embolotherapy without performing a biopsy and angiographic misinterpretation may lead to an inappropriate treatment. Arteriovenous malformations usually show rapid draining of contrast agent whereas ASPS shows a delayed washout pattern [4]. However, it is not always possible to exclude arteriovenous malformation because a mixed high and low flow pattern may be present as a continuous spectrum of vascular malformations. MR imaging can help to distinguish between a highly vascular ASPS and an arteriovenous malformation, by demonstrating an abundant solid tissue component in addition to signal voids, whereas arteriovenous malformation has exclusively vascular components with scanty solid tissue components in the tumor and frequently has fibrofatty tissue with high signal on T1-weighted images within the mass. In our cases (nos. 4, 7) where angiography had been initially interpreted as arteriovenous malformations, MR imaging enabled the correct diagnosis of soft tissue sarcoma.

ASPS can affect bones by direct or metastatic spread [14, 15]. In such cases the differential diagnosis includes a primary bone tumor with large soft tissue mass, a soft tissue mass with invasion of adjacent bones, and metastases. Distant bony metastases are reported commonly in ASPS (55.6%), followed by angiosarcoma (50%), dedifferentiated liposarcoma (50%) and rhabdomyosarcoma (26.7%) [16]. Local bone metastasis is not uncommon in soft tissue sarcoma [16], particularly ASPS, but it has not been fully discussed previously. It is conceivable that local bone metastasis can develop as a result of tumor emboli transferred via venous channels. It is also of concern that a relatively large bone lesion is accompanied small satellite nodules. It is our view that when ASPS is considered a presumptive diagnosis, efforts should be made to detect local bone metastases, and as ASPS has a propensity for bone and lung metastases, whole-body bone scintigraphy and chest CT are required for staging.

There is no consensus with regard to the efficacy of chemotherapy or embolotherapy for ASPS. Of the four patients who were followed with MR imaging, one had extensive central tumor necrosis, which was thought to be effective, but three cases showed no change.

In conclusion, increased signal compared with muscle on T1-weighted images and numerous signal voids on MR imaging are highly suggestive of ASPS, and the presence of a soft tissue mass should differentiate ASPS from arteriovenous malformation. Local bone metastases in ASPS are not uncommon.

www.manaraa.com

المنارة للاستشارات

**Table 2** Imaging findings of the patients (*AV* arteriovenous, *HmH* homogeneously high, *HtH* heterogeneously high)

| Case no. | T1-weighted image | T2-weighted image | Contrast-enhanced T1-weighted image | Signal void | Local bone lesion | Tumor margination | Angiography | MRI follow-up |
|---|---|---|---|---|---|---|---|---|
| 1 | HtH | HtH | HmH | Yes | No | Good | Hypervascularity, AV shunting, delayed washout | Central necrosis at 3 months after embolization and chemotherapy |
| 2 | HtH | HtH | HtH | Yes | No | Poor | | |
| 3 | HtH | HtH | HtH | Yes | Direct invasion; fibula | Poor | | |
| 4 | HtH | HtH | HtH | Yes | | Relatively good | Hypervascularity, AV shunting, delayed washout | No changes at 2 months after chemotherapy |
| 4 | HtH | HtH | HtH | No | Local metastasis to the femur with two satellite lesions | Good | | |
| 5 | HtH | HtH | HtH | Yes | Local metastasis to the femur | Good | Hypervascularity, AV shunting, delayed washout | No changes 2 months after chemotherapy |
| 6 | HtH | HtH | HtH | No | Direct invasion; skull | Good | | |
| 7 | HmH | HmH | HmH | Yes | No | Good | Hypervascularity, AV shunting, delayed washout | No changes at 6 months after embolization and chemotherapy |
| 8 | HmH | HtH | HmH | No | No | Relatively good | | |
| 9 | HmH | HmH | HmH | No | No | Relatively good | | |
| 10 | HtH | HtH | HtH | Yes | No | Relatively good | | |



www.manaraa.com

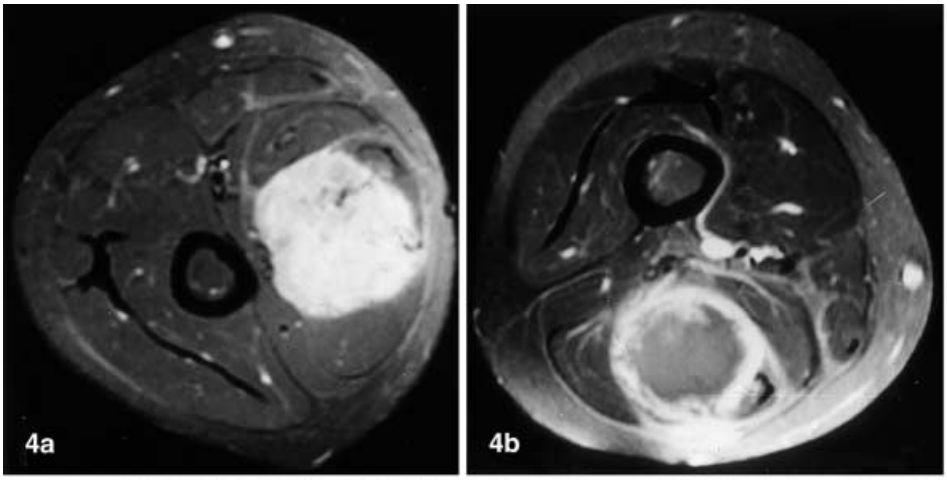


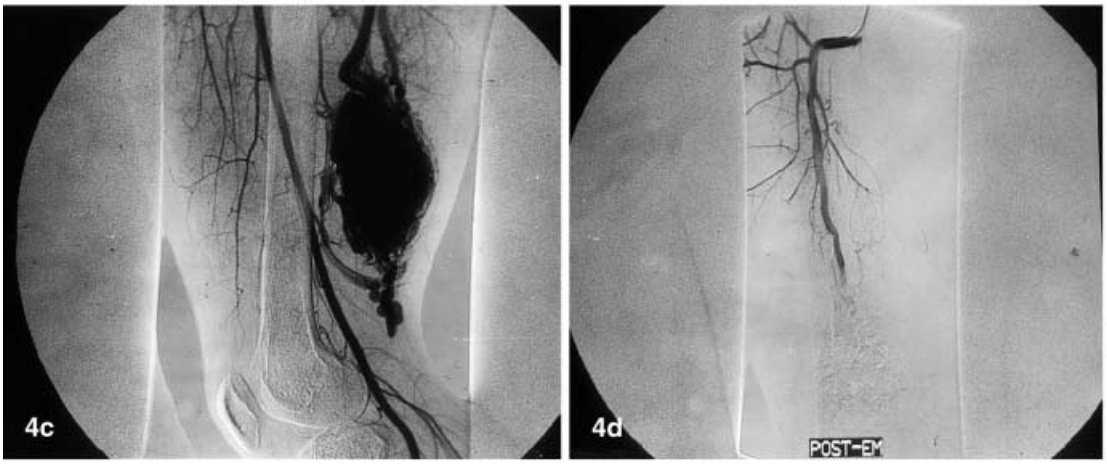


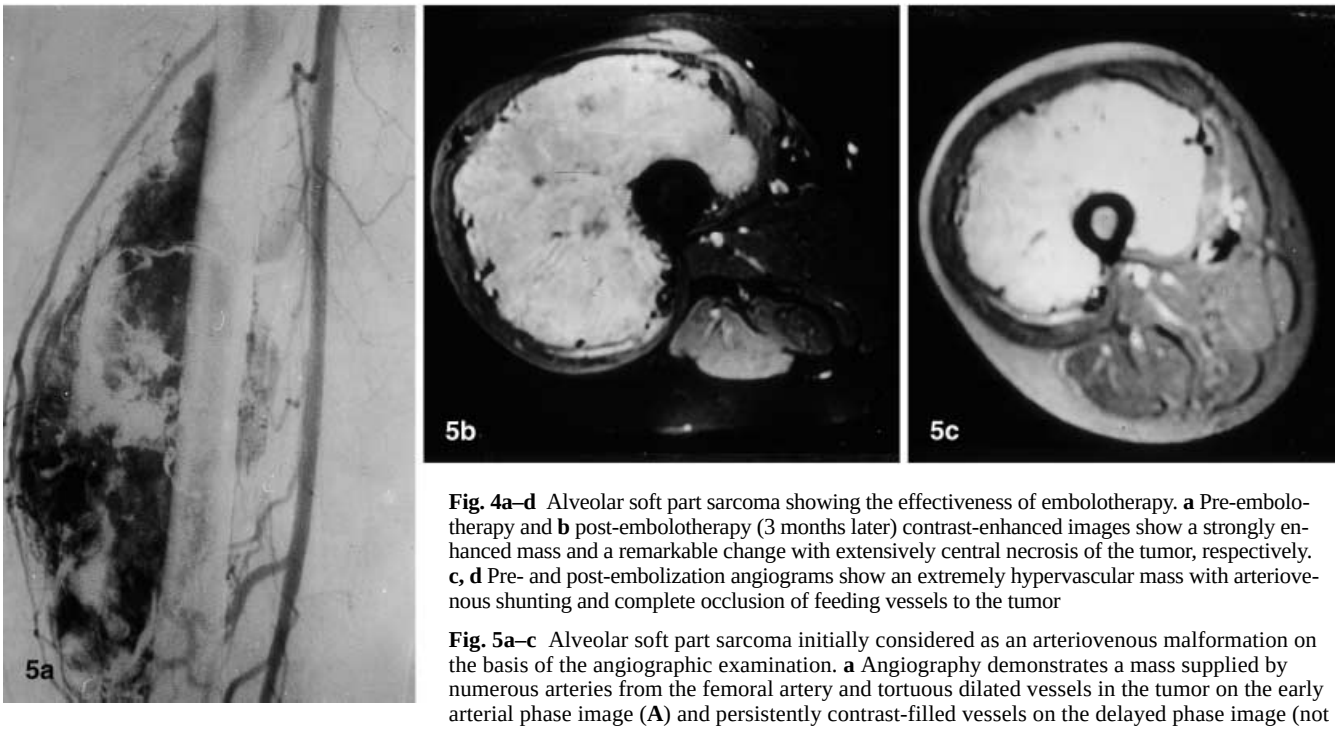


**Fig. 4a–d** Alveolar soft part sarcoma showing the effectiveness of embolotherapy. **a** Pre-embolotherapy and **b** post-embolotherapy (3 months later) contrast-enhanced images show a strongly enhanced mass and a remarkable change with extensively central necrosis of the tumor, respectively. **c, d** Pre- and post-embolization angiograms show an extremely hypervascular mass with arteriovenous shunting and complete occlusion of feeding vessels to the tumor

**Fig. 5a–c** Alveolar soft part sarcoma initially considered as an arteriovenous malformation on the basis of the angiographic examination. **a** Angiography demonstrates a mass supplied by numerous arteries from the femoral artery and tortuous dilated vessels in the tumor on the early arterial phase image (**A**) and persistently contrast-filled vessels on the delayed phase image (not shown). **b, c** Pre- and Post-embolization (six months later). T1-weighted fat-saturation post-contrast image show a relatively homogeneously enhanced mass

www.manaraa.com

## References


1. Christopherson WM, Foote FW Jr, Stewart FW. Alveolar soft-part sarcoma: structurally characteristic tumors of uncertain histogenesis. Cancer 1952; 5:100–111.
2. Enzinger FM, Weiss SW. Soft tissue tumors, 3rd edn. St Louis: CV Mosby, 1995:1067–1074.
3. Lorigan JG, O'Keeffe FN, Evans HL, Wallace S. The radiologic manifestations of alveolar soft-part sarcoma. AJR 1989; 153:335–339.
4. Iwamoto Y, Morimoto N, Chuman H, Shimohara N, Sugioka Y. The role of MR imaging in the diagnosis of alveolar soft part sarcoma: a report of 10 cases. Skeletal Radiol 1995; 24:267–270.
5. Lieberman PH, Brennan MF, Kimmel M, Erlandson RA, Garin-Chesa P, Flehinger BY. Alveolar soft part sarcoma: a clinicopathologic study of half century. Cancer 1989; 63:1–13.
6. Nakashima Y, Kotoura Y, Kasakura K, Yamamuro T, Amitani R, Ohdera K. Alveolar soft-part sarcoma a report of ten cases. Clin Orthop 1993; 294:259–266.
7. Evans HL. Alveolar soft-part sarcoma: a study of 13 typical examples and one with a histologically atypical component. Cancer 1985; 55:912–917.
8. Bridge JA, Sandberg AA. Cytogenetic and molecular genetic techniques as adjunctive approaches in the diagnosis of bone and soft tissue tumors. Skeletal Radiol 2000; 29:249–258.
9. Daly BD, Cheung H, Gaines PA, Bradley MJ, Metreweli C. Imaging of alveolar soft part sarcoma. Clin Radiol 1992; 46:253–256.
10. De Beuckeleer LH, De Schepper AM, Vandevenne JE, et al. MR imaging of clear cell sarcoma (malignant melanoma of the soft tissue parts): a multicenter correlative MRI-pathology study of 21 cases and literature review. Skeletal Radiol 2000; 29:187–195.
11. Dobson MJ, Hartley WJ, Ashleigh R, Watson Y, Hawnaur JM. MR angiography and MR imaging of symptomatic vascular malformations. Clin Radiol 1997; 52:595–602.
12. Temple HT, Scully SP, O'Keefe RJ, Rosenthal DI, Mankin HJ. Clinical presentation of alveolar soft part sarcoma. Clin Orthop 1994; 300:213–218.
13. Lo CM, Yeung HY, Siu KF. Misdiagnosed localized arteriovenous malformation. J Vasc Surg 1987; 6:419–421.
14. Aluigi P, Sangiorgi L, Picci P. Alveolar soft part sarcoma. Skeletal Radiol 1996; 25:400–402.
15. Hermann G, Abdelwahab IF, Klein MJ, Kenan S, Lewis MM. Case report 796. Alveolar soft part sarcoma. Skeletal Radiol 1993; 22:386–389.
16. Yoshikawa H, Ueda T, Mori S, et al. Skeletal metastases from soft-tissue sarcomas. J Bone Joint Surg Br 1997; 79:548–552.


المنارة للاستشارات
www.manaraa.com